Reactions of Iodomalonic Acid, Diiodomalonic Acid, and Other Organics in the Briggs−Rauscher Oscillating System

Stanley D. Furrow* and David J. Aurentz

Penn State Berks College, The Pennsylvania State University, Reading, Pennsylvania 19610

Received: December 3, 2009; Revised Manuscript Received: January 19, 2010

It was found that oxalic acid is one of the main products in the Briggs−Rauscher oscillating reaction. In nonoscillating solutions, oxidation of iodomalonic acid and/or diiodomalonic acid by Fenton-type reactions also produced oxalic acid as well as I_2. Mesoxalic acid yielded oxalic acid under similar conditions. Tartronic acid was nearly inert to Fenton-type reactions; however, tartronic acid was oxidized by iodate and iodine to mesoxalic acid, which in turn could form oxalic acid in the presence of H_2O_2 plus catalyst. Iodotartronic acid appeared to be a short-lived but significant intermediate, thus both tartronic acid and mesoxalic acid are possible intermediates. Glycolic acid and glyoxylic acid are not intermediates in the oxidation of iodomalonic acid, since they in turn produce formic acid under similar nonoscillating conditions.

Introduction

The Briggs−Rauscher (BR) oscillating system[1] (acid, H_2O_2, KIO_3, $MnSO_4$, malonic acid (MA), and starch) is a popular demonstration because of its spectacular color changes from clear to pale yellow to blue, then repetition every few seconds for several minutes, as I_2 and I^- are alternately produced and consumed. Skeleton models have been proposed,[2−8] but in general their simulations are not in quantitative agreement with experiment. As a first approximation, the models assume an overall reaction

$$H^+ + 2H_2O_2 + CH_2(CO_2H)_2 + IO_3^- \rightarrow ICH(CO_2H)_2 + 2O_2 + 3\,H_2O$$

with an unknown fraction of H_2O_2 decomposition,

$$2\,H_2O_2 \rightarrow 2\,H_2O + O_2$$

I_2 is produced by the overall process

$$5H_2O_2 + 2H^+ + 2IO_3^- \xrightarrow[\text{catalyst}]{Mn^{2+}\text{ or }Ce^{3+}} I_2 + 5O_2 + 6H_2O$$

This process is assumed to generate the radicals HOO• and IO_2• as well as nonradical intermediates HOIO and HOI. All of these species are potential reactants with any organic species present, whether malonic acid or its derivatives, or with perturbing agents to the BR reaction such as ferroin,[9] ascorbic acid,[10] diphenols, or other antioxidants.[11−13] It has been assumed that the inhibiting action of these perturbing agents is mainly due to interactions with radicals. They may, however, also interact with iodinated malonic acid products.

I_2 is consumed by the process

$$H^+ + IO_3^- + 2I_2 + 5CH_2(CO_2H)_2 \rightarrow 5ICH(CO_2H)_2 + 3H_2O$$

Malonic acid (MA) reacts with I_2 via an enol mechanism,[14] and iodomalonic acid (IMA) can react similarly to form diiodomalonic acid (I_2MA). The second iodination of IMA is not included in the skeleton mechanisms.

The skeleton models assume that IMA is an inert product, or that IMA contributions to the oscillations are relatively minor. Vanag[15] has suggested that iodinated products do have a roll in the oscillations. Recently Szabó et.al.[16] have expanded on that theme, and have shown that CO_2 and CO are evolved. Muntean et al.[17] have shown that Fenton-like radical attack on IMA is responsible for most of the CO_2 and CO evolution. Other evidence that IMA plays an active roll is the shortening of the induction period when IMA is added to the mixture. In the oscillating system $[H_2SO_4] = 0.10$ M, $[KIO_3] = 0.010$ M, $[MnSO_4] = 0.010$ M, $[MA] = 0.050$ M, $[H_2O_2] = 0.80$ M, the induction period is reduced from 54 to 0 s by the introduction of 0.0040 M [KI], and waiting for I_2 to clear, forming 0.0060 M IMA. Recently Lawson et al.[12] have shown that build-up of IMA shortens the inhibitory period when a BR reaction is perturbed by resorcinol.

This work focuses on some of the reactions of IMA and I_2MA and other possible degradation/oxidation products of those compounds, in particular as to whether the final products in solution are oxalic acid (OA) or formic acid (FA). Following the lead of Hansen, Ruoff and co-workers[18] on the Belousov−Zhabotinsky (BZ) oscillating system,[19] nuclear magnetic resonance (NMR) spectroscopy was used to identify products of the BR oscillating system and some of the subsystems. Some possible intermediates/products from oxidation, decarboxylation or decarbonylation are listed in Chart 1.

Experimental Methods

NMR spectroscopy was performed at ambient temperature on a 300 MHz Bruker Avance MicroBay spectrometer. The instrument was equipped with a 5 mm H−X ATM broadband probe and a deuterium lock channel. All spectra were collected

* To whom correspondence should be addressed. E-mail: f13@psu.edu.

10.1021/jp911492f
Published on Web 02/02/2010

CHART 1: Possible Intermediates and/or Products from Oxidation, Decarboxylation, or Decarbonylation of the BR Oscillating System

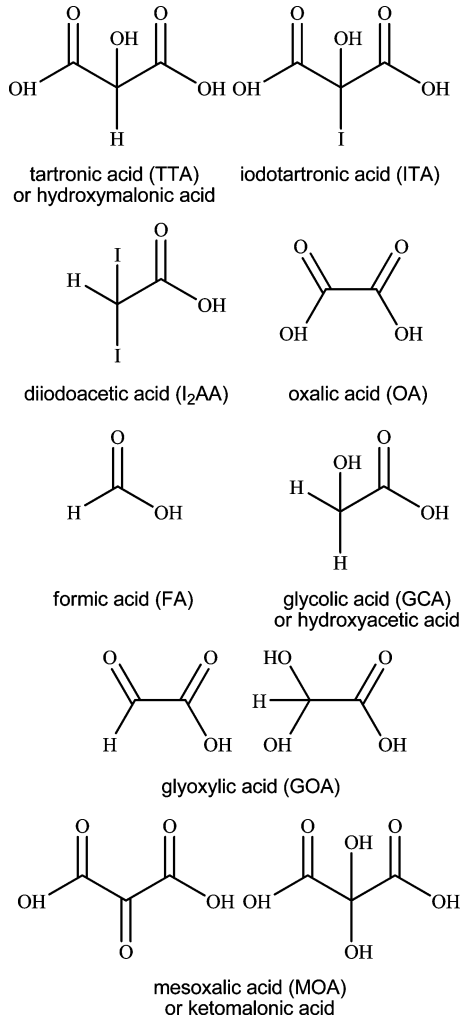

under standard conditions employing excitation field strengths for ^1H and ^{13}C of 18.5 and 33.3 kHz, respectively. All ^{13}C spectra were collected using WALTZ-16 proton decoupling.[20] UV−visible spectroscopy was done on a Shimadzu model 1501 with a thermostatted cell compartment at 25.0 °C.

Chemicals. H_2O_2 (30%) was Fisher certified ACS, stabilizer free. 70% $HClO_4$, KIO_3, and $MnSO_4 \cdot H_2O$ were Baker reagent grade and were used without further purification. Malonic acid from Aldrich was recrystallized twice from water. Tartronic acid (Alfa Aesar, 98%), sodium mesoxalate (Aldrich, 98%), glyoxylic acid monohydrate (Aldrich 98%), glycolic acid (Sigma), and cerous nitrate (Anachemia, reagent grade) were used as received. I_2AA was prepared from MA with HIO_3 following the procedure of Cobb.[21] IMA was prepared as the dipotassium salt[22] or in situ.[23] I_2MA was prepared from MA + I_2 + HIO_3 in formic acid.[21] Deionized water was used to make all solutions.

Results and Discussion

Peak Identification for ^1H and ^{13}C NMR. Table 1 shows the peaks for the major species in this study. The ^1H peaks vary as much as ±0.1 ppm with different samples, depending on acidity and amount of D_2O in the sample. Usually ^{13}C peaks were reproducible (with different samples) within ±0.5 ppm. Most samples contained 10−15% D_2O. Solution-state ^1H and ^{13}C NMR experiments were used to look for products within a few minutes to approximately an hour after oscillations stop (and bubbling slows down). There are several limitations with ^1H NMR: IMA at 5.1 ppm and TTA at 4.9 ppm are near the water peak, and often obscured; I_2MA, oxalic acid, and mesoxalic acid have no nonacidic protons; Mn^{2+} broadens the water peak substantially and degrades the ^{13}C spectrum. Water suppression[24] can help with sensitivity away from the water peak, but desired signals from IMA and TTA were suppressed as well, so suppression did not resolve all peaks. ^{13}C spectra are more discerning but require higher concentrations or substantially longer acquisition times. Ce^{3+} catalyst has less broadening effect on the peaks than Mn^{2+}catalyst, so Ce^{3+} was substituted for Mn^{2+} in some analyses.

TABLE 1: NMR Peaks for Selected Compounds

compound	^1H peak (ppm)	^{13}C peaks (ppm)[a]
I_2MA		170, −11
IMA	5.1	171, 15.5
MA	3.4	171, 40.7
TTA	4.9	171, 71
MOA		173.5, 90
GOA	5.3	172.9, 86
GCA	4.1	175.3, 58.9
I_2AA	5.5	168.9, −38
OA		161.6
FA	8.2	165.3
CO_2		124

[a] Highly iodinated carbons have peaks upfield of normal reference compounds for ^{13}C and have negative chemical shift values.

End Products from the BR Reaction. The products at the immediate end of oscillations are strongly affected by the initial concentrations. The ratio of [MA] to [IO_3^-] is especially important in determining whether [I_2] increases dramatically at the end, enough to precipitate solid I_2, or whether [I_2] and [I^-] remain low for an extended time. The I_2 presumably comes from rapid decomposition of iodinated products.[15] Higher [H_2O_2], [catalyst], and total [acid] also increase the probability of high [I_2], but to a lesser extent. This work focuses on mixtures with a relatively high ratio (>2:1) of [MA] to [IO_3^-] where oscillations end with a clear solution. This reduces complications due to I_2MA formed during the oscillations and to precipitating I_2. Reactions continue in the solution certainly for the next hour, and then for at least several days, with I_2 often being released, H_2O_2 decomposing, and organic matter being oxidized.

In the UV, during oscillations, absorbance increases in the region 300−360 nm,[15] indicating iodinated products (and/or I_3^-); noniodinated organics are completely hidden by absorbance from H_2O_2 and IO_3^-. NMR can give much more specific information.

Typical oscillating mixtures used in this work had $[HClO_4]_0$ = 0.10 M, $[KIO_3]_0$ = 0.020 M, $[Ce(NO_3)_3]_0$ = 0.00667 M, $[MA]_0$ = 0.050 M, $[H_2O_2]_0$ = 1.0 M, [acetic acid (AA)]$_0$ = 0.022 M as an internal reference peak for NMR. Figure 1 shows a trace with an iodide-selective electrode vs Ag−AgCl with a KNO_3 salt bridge. Samples for NMR analyses were taken after cessation of oscillations.

In general, the major organic species present immediately after oscillations are MA, IMA, and oxalic acid. When Ce^{3+} is used as a catalyst, a white precipitate, $Ce_2(C_2O_4)_3$, (or the hydrate) often forms during the oscillatory regime, thereby decreasing the catalyst concentration and lessening the overall reaction rate. The precipitate can be separated and dissolved in H_2SO_4, and the oxalate is identified with ^{13}C NMR. With Mn^{2+} as a catalyst, addition of saturated $CaCl_2$ and lowering the pH

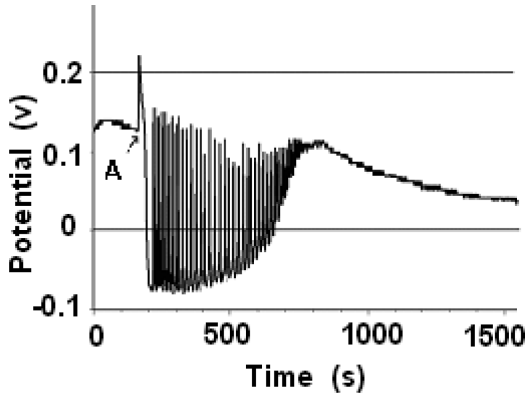

Figure 1. Iodide-selective electrode potential vs time for an oscillating mixture (high $[I^-]$ is at lower potentials). $[HClO_4]_0 = 0.10$ M, $[KIO_3]_0 = 0.020$ M, $[Ce(NO_3)_3]_0 = 0.00667$ M, $[MA]_0 = 0.050$ M, $[H_2O_2]_0 = 1.0$ M, $[AA]_0 = 0.022$ M as an internal NMR reference peak. A: H_2O_2 added.

with sodium acetate causes precipitation of CaC_2O_4, which can be separated, redissolved in acid, and titrated with $KMnO_4$ or identified with ^{13}C NMR.

Formic acid (FA) is not seen after oscillations in typical oscillators at a detection level in ^1H NMR of approximately 2×10^{-4} M. An oscillating mixture with $[H_2SO_4]_0 = 0.10$ M, $[KIO_3]_0 = 0.020$ M, $[MnSO_4]_0 = 0.0067$ M, $[MA]_0 = 0.050$ M, $[H_2O_2]_0 = 1.33$ M, and $[AA]_0 = 0.022$ M (as a reference) compared to a similar mixture with $[FA]_0 = 0.020$ M has the same induction period (40 ± 2 s) and the same length of oscillations (505 ± 5 s). A sample from the oscillator with formic acid was withdrawn before addition of H_2O_2 and compared with another sample after oscillations. The ratio of [AA] to [FA] was unchanged. Using ^1H NMR, both the AA peak at 2.09 ppm and the FA peak at 8.23 ppm are completely resolved from the broadened water peak, allowing for quantitative comparison.

A typical oscillator was perturbed with 0.022 M GOA and the induction period and length of oscillations was essentially unchanged; formic acid was produced. This indicates that GOA is not an intermediate in the breakdown of IMA. When a similar oscillator was perturbed with 0.023 M GCA, again there was little effect in oscillations, and most of the GCA was present at the end of oscillations. Likewise, GCA can be ruled out as an important intermediate.

IMA Reactions. IMA is photosensitive, so spectrophotometric studies must be made intermittently to minimize degradation. IMA does not react significantly with acid, acidic IO_3^-, Mn^{2+}, or H_2O_2 on a time scale of approximately 1 h. There is an autocatalytic reaction with H_2O_2 and Mn^{2+} or Ce^{3+} catalyst, sometimes after a significant induction period, with I_2 and I_3^- as products (This is a Fenton-type reaction). The absorbance at 462 nm is mainly due to I_2; absorbance at 352 nm is mainly from I_3^-. Much of the iodine in IMA must be released as I^-. Decrease in the absorbance at 352 nm after its maximum is from oxidation of I^- and I_3^- by H_2O_2. For mixtures where $[IMA]_0$ is 0.0020 M or less, approximately 90% of the iodine in IMA is eventually returned as I_2. A typical run is shown in Figure 2. Mixtures with $[IMA]_0 > 0.0040$ M behave differently and need further investigation.

The main organic product is oxalic acid (seen in ^{13}C NMR); thus, an approximation for the main overall reaction is

$$2\,ICH(CO_2H)_2 + 5H_2O_2 \rightarrow I_2 + 2H_2C_2O_4 + 2CO_2 + 6\,H_2O$$

Without Mn^{2+} or Ce^{3+} present, the reaction is much slower. There was no I_2 absorbance for an observation time of 11/2 h with $[HClO_4] = 0.10$M, $[IMA] = 0.0021$ M, and $[H_2O_2] = 1.0$M. With metal catalyst, the induction time is erratic and not reproducible. The induction time is usually different for portions of a solution that are separated after mixing, even though they are kept in darkness and at constant temperature. The build-up of radical species is presumably affected by slight differences in environment, including stirring rate and container size.

During reactions when Mn^{2+} is present, the reaction speed is somewhat faster with increasing $[Mn^{2+}]$, reflected in higher maximum slope, d(Abs 462)/dt. The time to half-maximum in $[I_2]$ is generally shorter with higher $[Mn^{2+}]$, although the induction time is erratic, especially at low $[Mn^{2+}]$. The results of several reactions starting with different concentrations of Mn^{2+} are shown in Table 2.

In general, the iodine in IMA can act as either I^+ or I^-, depending on the reagent. Reducing agents seem to remove iodine as I^+, producing malonic acid and I_2 or I^-. Oxidizing agents and metal ions such as Hg^{2+} remove iodine as I^- and produce tartronic acid and HgI_2 or I_2. Several reactants have been included in the following sections to illustrate both possibilities.

IMA + I⁻. The kinetics of this reaction have been studied by Leopold and Haim.[14] Enolization of MA was studied by Ruoff et al.[25]

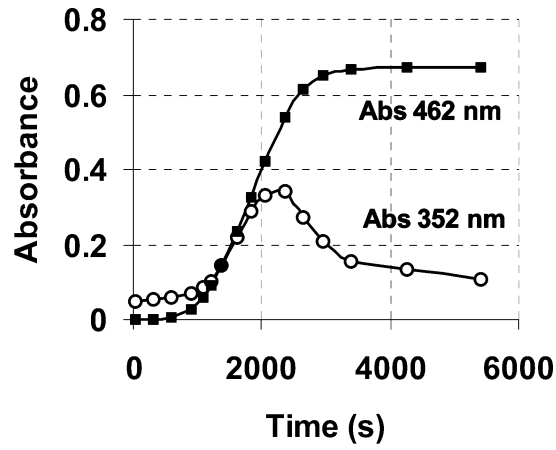

Figure 2. Absorbance at 462 and 352 nm vs time for $[HClO_4]_0 = 0.10$ M, $[H_2O_2]_0 = 1.0$ M, $[MnSO_4]_0 = 0.0020$ M, $[IMA]_0 = 0.0020$ M.

TABLE 2: Effect of $[MnSO_4]$ on IMA Decomposition[a]

$[MnSO_4]$ ($M \times 10^3$)	time (s)[b]	max d(Abs462)/dt ($M^{-1}cm^{-1}s^{-1} \times 10^4$)
0.50	3570	4.0
1.00	1850	4.5
2.00	1140	5.0
3.00	730	5.0
5.00	990	5.5
10.0	995	5.5

[a] $[HClO_4] = 0.10$ M, $[IMA] = 2.00$ M $\times 10^{-3}$ M, and $[H_2O_2] = 1.0$ M in all solutions. [b] Time from mixing to 1/2 maximum in $[I_2]$.

$$H^+ + I^- + ICH(CO_2H)_2 \rightleftharpoons CH_2(CO_2H)_2 + I_2$$

IMA + Reducing Agent (Ascorbic Acid). This reaction is finished by the time ^{1}H NMR measurements can be made, but a decrease in IMA and an increase in MA peaks were observed. Both the ascorbic acid and the oxidation product peaks were distinct and resolvable when analyzed by ^{1}H NMR.

$$ICH(CO_2H)_2 + 2H^+ + \text{ascorbic acid} \rightarrow CH_2(CO_2H)_2 + H^+ + I^- + \text{dehydroascorbic acid}$$

IMA as Iodinating Agent with Resorcinol. Peaks from excess reactant and both products were present in ^{1}H and ^{13}C NMR.[26]

$$IMA + \text{resorcinol (excess)} \rightarrow \text{iodoresorcinol} + MA$$

IMA + I_2. Iodide must be removed to move the equilibrium to the right.

$$ICH(CO_2H)_2 + I_2 \rightleftharpoons CI_2(CO_2H)_2 + H^+ + I^-$$

When IO_3^- is present, the process is:

$$5ICH(CO_2H)_2 + 2I_2 + H^+ + IO_3^- \rightleftharpoons 5CI_2(CO_2H)_2 + 3H_2O$$

Both IMA and I_2MA are photosensitive, so measurements in a continuous spectrophotometer beam were distorted. Overhead lights cause decomposition, so mixtures must be prepared in diffuse light. The product, I_2MA, undergoes decarboxylation to I_2AA and reacts with any MA present to form IMA.[13]

IMA + Hg^{2+}. The reaction was slow until warmed. After filtration of HgI_2, both MA and MOA were found when analyzed by ^{13}C NMR instead of the expected TTA. Apparently disproportionation occurred during or just after deiodination.

$$2H_2O + 2ICH(CO_2H)_2 + Hg^{2+} \rightarrow C(OH)_2(CO_2H)_2 + CH_2(CO_2H)_2 + HgI_2(s) + 2H^+$$

I_2MA Reactions. I_2MA is much more reactive than IMA and readily releases I_2 and I^-. Onel et al.[13] have characterized several reactions of I_2MA, using I_2MA prepared in situ from MA + $NaIO_3$ + KI in acid. In this work I_2MA prepared by the method of Cobb[21] (HIO_3 + KI + MA in FA) was used. I_2MA precipitated out of solution.

I_2MA Decarboxylation. This reaction has been studied previously.[13]

$$CI_2(CO_2H)_2 \rightarrow HCI_2CO_2H(I_2AA) + CO_2$$

I_2MA + Excess I^-. See IMA + I_2 above.

$$H^+ + 2I^- + CI_2(CO_2H)_2 \rightleftharpoons CH_2(CO_2H)_2 + 2I_2$$

I_2MA + Excess Reducing Agent (Ascorbic Acid, HNO_2, $S_2O_3^{2-}$). These reactions are finished by the time NMR measurements can be made, but an increase in the MA peak can be seen in ^{1}H NMR. Both ascorbic acid and its oxidation product, dehydroascorbic acid, have peaks in ^{1}H NMR.

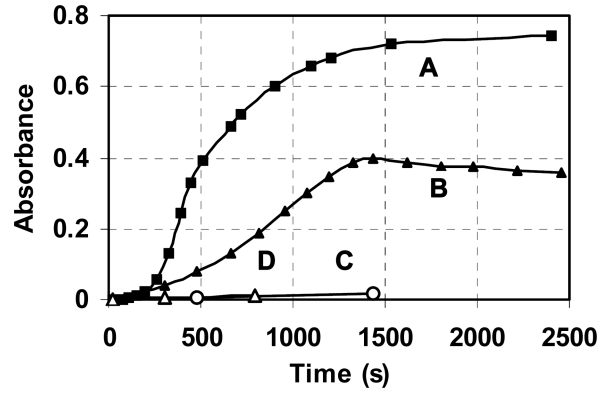

Figure 3. Absorbance at 462 nm vs time for I_2MA reactions in several mixtures. All mixtures: $[HClO_4]_0 = 0.10$ M, $[I_2MA]_0 = 0.0013$ M; A: $[H_2O_2]_0 = 1.0$ M, $[MnSO_4]_0 = 0.00050$ M; B: $[H_2O_2]_0 = 1.0$ M; C: (open circles) only $HClO_4$ and I_2MA; D: (open triangles) $[KIO_3]_0 = 0.010$ M, $[MnSO_4]_0 = 0.010$ M.

$$CI_2(CO_2H)_2 + 2H^+ + 4e^- \rightarrow CH_2(CO_2H)_2 + 2I^-$$

I_2MA + Hg^{2+}. Solid I_2MA was added to a solution of $HgSO_4$ in 3 M H_2SO_4. After approximately 1 h at 40 °C, then filtration of HgI_2, MOA was the only major peak in ^{13}C NMR.

$$2H_2O + Hg^{2+} + CI_2(CO_2H)_2 \rightarrow C(OH)_2(CO_2H)_2 + 2H^+ + HgI_2(s)$$

I_2MA + H_2O_2 + Ce(III) or Mn(II). After an initial delay (at low [catalyst]), I_2MA undergoes a rapid autocatalytic deiodination when both H_2O_2 and either Ce(III) or Mn(II) are present. Following by UV spectrophotometry reveals that more than 80% of the iodine in I_2MA is liberated as I^- or I_3^-, then oxidized to I_2 by H_2O_2. Figure 3 compares various subsets. ^{13}C NMR analysis of the filtered solution (to remove solid I_2) showed oxalic acid as the major remaining organic component, with a small amount of I_2AA.

There is very little reaction of I_2MA with either $MnSO_4$ or KIO_3, but moderate reaction with H_2O_2. With both $MnSO_4$ and H_2O_2 present the reaction is much faster. The effect of $MnSO_4$ is shown in Figure 4.

When $[MnSO_4]$ is approximately 0.0050 M, in the region of its concentration in typical oscillating mixtures, the reaction is substantially complete by the time a cuvette can be placed in the spectrophotometer. Although IMA can be a substrate for oscillations,[27] indicating some I_2MA forming, it seems that I_2MA cannot build up to any great extent in an oscillating mixture. A summary of nonoscillating runs is shown in Table 3.

Other Organics with H_2O_2 and Mn^{2+} or Ce^{3+}. Several possible intermediates in the oxidation of IMA and I_2MA have been studied in an acidic Fenton-like environment with H_2O_2 and metal catalyst. H_2SO_4 or $HClO_4$ concentrations were approximately 0.1 M; $[H_2O_2] = 1.0$ M; $[Ce^{3+}]$ or $[Mn^{2+}] = 0.007$ M.

MOA is rapidly oxidized to OA and CO_2.

$$3C(OH)_2(CO_2H)_2 + 3H_2O_2 + 2Ce^{3+} \rightarrow Ce_2(C_2O_4)_3 + 3CO_2 + 6H_2O + 6H^+$$

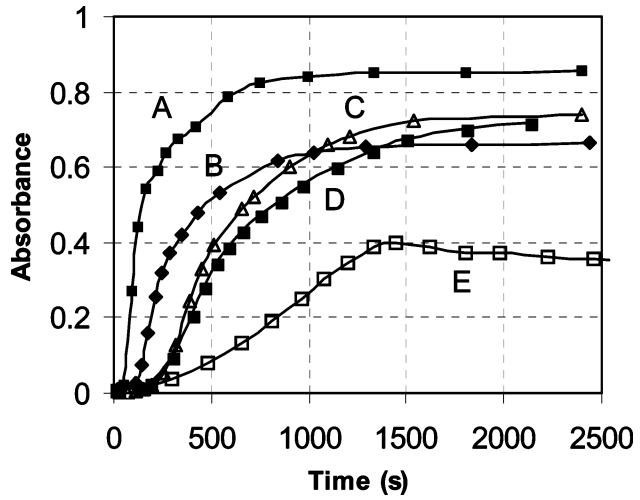

Figure 4. Absorbance at 462 nm vs time; I_2MA decomposition with $[H_2O_2]$ and different $[MnSO_4]$. All: $[HClO_4]_0 = 0.10$ M, $[H_2O_2]_0 = 1.0$ M. $[MnSO_4]$: A, 5.0×10^{-4} M; B, 2.0×10^{-4} M; C, 1.0×10^{-4} M; D, 0.50×10^{-4} M; E, 0 M.

TABLE 3: I_2MA Decomposition[a]

method	$[I_2MA]$ ($M \times 10^3$)	$[H_2O_2]$ (M)	$[MnSO_4]$ ($M \times 10^3$)	approximate $t_{1/2}$[b] (s)
UV	1.4	1.0	10	<60
UV	1.4	0.50	5.0	<60
UV	1.3	0.50	2.7	49
UV	1.3	0.50	1.3	83
UV	1.3	0.50	0.50	135
UV	1.3	1.0	0.50	120
UV	1.3	1.0	0.20	270
UV	1.4	1.0	0.10	480
UV	1.4	1.0	0.050	540
I^- electrode	1.49	1.0	5.0	50
I^- electrode	1.35	1.0	2.0	240
I^- electrode	1.37	1.0	1.0	135
I^- electrode	1.50	1.0	2.0[c]	240
I^- electrode	0.072	1.0	1.0[c]	200

[a] $[HClO_4] = 0.10$ M in all solutions. [b] Time for $[I_2]$ or $[I^-]$ to reach half-maximum. [c] $Ce(NO_3)_3$ instead of $MnSO_4$.

At $[H_2SO_4] = 0.10$M, $[Ce(NO_3)_3] = 0.0050$M, $[H_2O_2] = 1.0$M, bubbling set in rapidly along with precipitation of $Ce_2(C_2O_4)_3$. In about 10 min the bubbling subsided, the solution was filtered and a ^{13}C spectrum showed only OA. MOA entirely disappeared.

TTA is nearly inert on a time scale of several days. If, however, even small amounts of iodine (as IO_3^-, I_2, or I^-) are present, TTA is oxidized to MOA which then is oxidized to OA and CO_2.

GOA is oxidized to FA and CO_2 within a few minutes.

$$HC(OH)_2CO_2H + H_2O_2(+\text{catalyst}) \rightarrow H_2CO + CO_2 + 2H_2O$$

GCA is oxidized to FA and CO_2 in a short time (tens of minutes) and GOA was seen via ^{13}C NMR as an intermediate.

$$CH_2OHCO_2H + H_2O_2(+\text{catalyst}) \rightarrow H_2CO + CO_2 + 2H_2O$$

OA is very slowly oxidized to CO_2, on a scale of two or three days.

$$(CO_2H)_2 + H_2O_2(+\text{catalyst}) \rightarrow 2CO_2 + H_2O$$

FA is not appreciably oxidized in a time frame of a few weeks.

TTA and MOA Reactions with I_2 and/or IO_3^-. Because both of these species are possible oxidation intermediates, it is of interest to examine their reactions with either I_2 or IO_3^- or both; I_2 or IO_3^- are present during oscillations.

MOA + I_2 + IO_3^-. An acidic mixture of the three species ($[HClO_4]_0 = 0.10$M, $[KIO_3]_0 = 0.010$M, $[I_2]_0 = 5.6 \times 10^{-4}$M, and $[MOA]_0 = 0.10$M) was essentially unchanged at 462 nm (I_2 peak absorbance) in 1.5 h. Thus MOA reaction with either I_2 or IO_3^- can be neglected.

TTA in D_2O. Observation of TTA in D_2O with ^1H NMR showed a decrease in peak intensity with time, confirming previous studies with bromine that an enol mechanism is involved.[28]

TTA + I_2. Run A. An acidic mixture ($[HClO_4] = 0.10$M, $[I_2] = 4.1 \times 10^{-4}$M, and $[TTA] = 0.0108$M) showed a steady decrease in absorbance at 462 nm and an increase to a maximum at 352 nm (I_3^- peak), and finally a decrease to near 0 at all wavelengths above 300 nm. TTA is oxidized; I_2 is reduced to I^-.

$$CH(OH)(CO_2H)_2 + I_2 + H_2O \rightarrow C(OH)_2(CO_2H)_2 + 2H^+ + 2I^- \quad \text{(S1)}$$

$$\text{TTA} \rightleftharpoons \text{enol} \quad \text{(S2)}$$

$$\text{enol} + I_2 \rightarrow ICOH(CO_2H)_2 + H^+ + I^- \quad \text{(S3)}$$

where $ICOH(CO_2H)_2$ is iodotartronic acid (ITA) or 2-hydroxy, 2-iodomalonic acid, ITA is expected to hydrolyze quickly.

$$ICOH(CO_2H)_2 + H_2O \rightarrow C(OH)_2(CO_2H)_2(MOA) + H^+ + I^- \quad \text{(S4)}$$

The triiodide equilibrium is important.

$$I_2 + I \rightleftharpoons I_3^- \quad \text{(S5)}$$

Assuming these reactions, it was possible to get a reasonable fit to the absorbance at 352 and 462 nm using the integration and curve fitting abilities of the *Copasi* simulation Program[29] to find forward and reverse constants for S2 (k_2 and k_{2r}), and k_4. (Values of k_{2r} and k_3 are not independent. The ratio k_3/k_{2r} is important). Figure 5 shows experimental and simulated results for 352 nm absorbance for the Run A; Figure 6 shows results for 462 nm absorbance for the same run. (Assuming that TTA + $I_2 \rightarrow$ MOA + 2 H^+ + 2I^- did not result in a reasonable fit; that is, ITA is required in the simulation). Rate laws and rate constants for all the steps used in the simulations are shown in Table 4. Extinction coefficients used are shown in Table 5.

TTA + H^+ + IO_3^-. Run B. An acidic mixture of TTA with KIO_3 ($[HClO_4]_0 = 0.10$M, $[KIO_3]_0 = 0.020$M, and $[TTA]_0 = 0.0393$M) had an increase of absorbance at 462 nm to 0.968 in 1.8 h. See Figure 7. In a separate ^{13}C NMR run ($[H_2SO_4]_0 =$

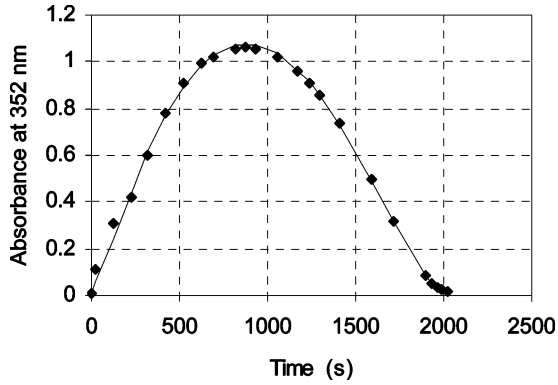

Figure 5. Absorbance at 352 nm (I_3^-) vs time for Run A: $[HClO_4]_0$ = 0.10 M, $[TTA]_0$ = 0.0108 M, $[I_2]_0$ = 0.00041 M. Diamonds, experimental; solid line, calculated. Mean standard deviation: 0.020.

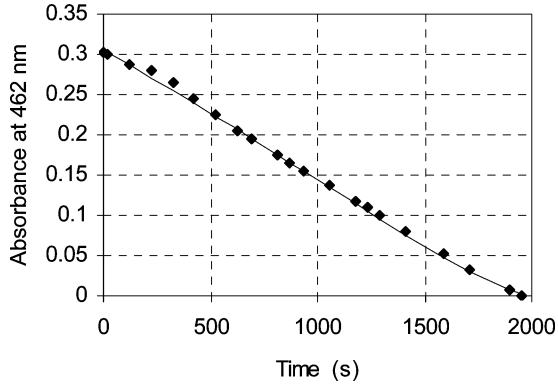

Figure 6. Absorbance at 462 nm (I_2) vs time for Run A: $[HClO_4]_0$ = 0.10 M, $[TTA]_0$ = 0.0108 M, $[I_2]_0$ = 0.00041 M. Diamonds, experimental; solid line, calculated. Mean standard deviation: 0.004.

0.10M, $[HIO_3]_0$ = 0.14M, and $[TTA]_0$ = 0.55M), the MOA peak at 91 ppm slowly increased and the TTA peak at 71 ppm decreased over several hours. The overall reaction is

$$6CHOH(CO_2H)_2\ (\text{excess}) + 2IO_3^- \rightarrow 6C(OH)_2(CO_2H)_2 + 2I^-$$

The reaction is relatively slow, several percent per hour, but not completely negligible. The following reactions were assumed to be involved.

$$H^+ + IO_3^- + TTA \rightarrow MOA + HOIO \qquad (S6)$$

$$TTA + HOIO \rightarrow MOA + HOI \qquad (S7)$$

Simulations showed that reaction S7 must be included to prevent an initial induction period. Something is needed to speed up removal of HOIO.

There are several reactions of I^- that would be involved when IO_3^- is present. The overall reaction (the Dushman[36] reaction) is

$$6H^+ + 5I^- + IO_3^- \rightarrow 3I_2 + 3H_2O$$

The following three reactions are subsets of the Dushman reaction; the first two, S8 and S9, come from the two steps in the rate law. The two steps are shown separately in Table 4.

$$2H^+ + I^- + IO_3^- \rightleftharpoons HOIO + HOI \qquad (S8)$$

$$3H^+ + 2I^- + IO_3^- \rightleftharpoons HOIO + I_2 + H_2O \qquad (S9)$$

$$H^+ + I^- + HOIO \rightleftharpoons 2HOI \qquad (S10)$$

$$H_2O + I_2 \rightleftharpoons H^+ + I^- + HOI \qquad (S11)$$

Rate constants for reactions S2 and S4 were first derived from the data in Figures 5 and 6 at the same time, assuming a literature value for k_3.[28]

Next, values for k_4, k_6, k_7, and k_8 were found from data in Run B, Figure 7. The value for k_7 was arbitrarily set within the range required to prevent clock-like behavior in the simulation. The value for k_4 (0.0052 ± 0.0005 M^{-1} s^{-1}) was reasonably close to that determined from Run A (0.0083 ± 0.0004 M^{-1} s^{-1}). The value for k_6 was 0.0039 ± 0.0001 M^{-1} s^{-1}. The constants k_4 and k_6 were then determined from Run C, Figure 8. (Details on Run C are in the following section). From these data, k_4 = 0.033 ± 0.009 M^{-1} s^{-1} and k_6 = 0.0022 ± 0.0002 M^{-1} s^{-1}. The two constants are inversely related: that is, a small increase in k_6 has the same effect as a larger decrease in k_4. In fact, when k_4 is forced at 0.0080 M^{-1} s^{-1}, k_6 becomes 0.0040 ± 0.0003 M^{-1} s^{-1}. Given the larger uncertainties from Run C, the values from Runs A and B were weighted more heavily in choosing values to use for simulations.

The values used for the simulations are presented in Table 4. The uncertainties in the rate constants in the table reflect differences derived from different data sets. The lines in all the figures were calculated from the constants in the table. There are some systematic differences between experiment and calculation that indicate the set of assumed reactions is incomplete or that some of the accepted rate constants may be in error. We believe the agreement is good enough to show that the TTA reaction with I_2 and IO_3^- can be reasonably modeled with the rate constants given.

TTA + I_2 + H^+ + IO_3^-. Run C. An acidic mixture ($[HClO_4]$ = 0.10M, $[KIO_3]$ = 0.010M, $[I_2]$ = 5.6 × 10^{-4}M, and [TTA] = 0.020M) showed an initial small decrease in absorbance at 462 nm, then a steady increase, significantly faster than the reaction above (Run B) with only TTA + HIO_3. TTA is oxidized; IO_3^- is reduced to I_2. See Figure 8.

$$5CH(OH)(CO_2H)_2 + 2H^+ + 2IO_3^- \rightarrow 5\ C(OH)_2(CO_2H)_2 + I_2 + H_2O$$

The reaction was stopped before solid I_2 precipitated. ITA has a half-life of up to approximately 100 s. It cannot be completely neglected in the oscillating mixture.

Comparison with the Belousov−Zhabotinsky (BZ) Reaction. The results above have some similarities to the results in the BZ reaction, in which malonic acid is also halogenated (with bromine) and then oxidized by Ce(IV) and oxybromine species. The pathways have been studied by Ruoff and co-workers,[25,37] by Gyorgi et. al,[38] and by Wittman, Noszticzius, et al.[28,39−41] They showed that the nonradical intermediates TTA, MOA, and

TABLE 4: Rate Laws used in Simulations[a]

	rate law or K_{eq}	$k_{forward}$ or K_{eq}	$k_{reverse}$	REF
S2	k_2[TTA] − k_{2r}[enol]	$(2.2 \pm 0.2) \times 10^{-5}$ s^{-1}	2.2 ± s^{-1}	this work[b]
S3	k_3[enol][I_2]	3×10^5 M^{-1} s^{-1}		28[c]
S4	k_4[ITA]	0.008 ± 0.004 s^{-1}		this work[d]
S5	[I_3^-]/[I_2][I^-]	715		30
		6.08×10^9 s^{-1}	8.5×10^6 $M^{-1}s^{-1}$	31[e]
S6	k_6[H^+][IO_3^-][TTA]	$(4 \pm 2) \times 10^{-3}$ M^{-2} s^{-1}		this work
S7	k_7[TTA][HOIO]	50 M^{-1} s^{-1}		this work[f]
S8	k_8[H^+]^2[IO_3^-][I^-] − k_{8r}[HOI][HOIO]	1200 M^{-3} s^{-1}	240 M^{-1} s^{-1}	32
S9	k_9[H^+]^2[IO_3^-][I^-]^2	4×10^8 M^{-4} s^{-1}		32
S10	k_{10}[I^-][HOIO] − k_{10r}[HOI]^2	5×10^9 M^{-1} s^{-1}	25 M^{-1} s^{-1}	33
S11	k_{11}[I_2]/[H^+] − k_{11r}[HOI][I^-]	0.0018 M^{-1} s^{1-}	3.6×10^9 M^{-1} s^{-1}	33

[a] Abbreviations: TTA, tartronic acid; ITA, iodotartronic acid. [b] Compare ref 28, $k_2 = 2.3 \times 10^{-5}$ s^{-1}, $k_{2r} = 1.5$ s^{-1} in 1 M H_2SO_4 at 20 °C. [c] From ref 28, $k = 3 \times 10^5$ s^{-1} in 1 M H_2SO_4 at 20 °C for Br_2 + enol. [d] Compare ref 28, $k = 1.5$ s^{-1} in 1 M H_2SO_4 at 20 °C for hydrolysis of bromotartronic acid. [e] $k_{reverse}$ from ref 31, $k_{forward}$ from 715 × $k_{reverse}$. [f] Arbitrary choice. Model is insensitive between 20 and 1000 M^{-1} s^{-1}.

TABLE 5: Extinction Coefficients Used for Simulations

substance	ϵ at 352 nm	ϵ at 462 nm	ref
I_2	18 M^{-1} cm^{-1}	746 M^{-1} cm^{-1}	34[a], 35[b]
I_3^-	26400 M^{-1} cm^{-1}	975 M^{-1} cm^{-1}	[a], 35[b]

[a] The extinction coefficients in the table are those of Awtrey and Connick[34] at 353 nm and at 460 nm. [b] Allen and Keefer[35] reported 20 $M^{-1}cm^{-1}$ and 26 400 $M^{-1}cm^{-1}$ at 352 nm and 742 M^{-1} cm^{-1} and 1030 M^{-1} cm^{-1} at 462 nm.

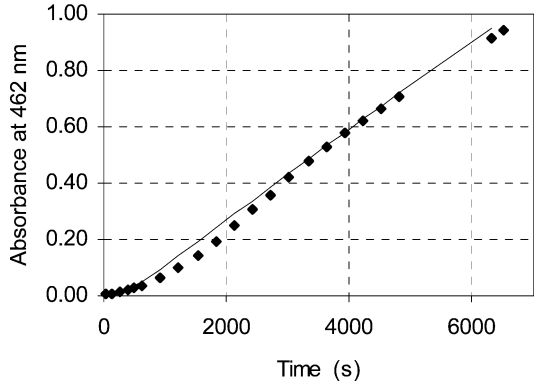

Figure 7. Absorbance at 462 nm vs time for Run B: $[HClO_4]_0 = 0.10$ M, $[TTA]_0 = 0.0393$ M, $[IO_3^-]_0 = 0.020$ M. Diamonds, experimental; solid line, calculated. Mean standard deviation: 0.017.

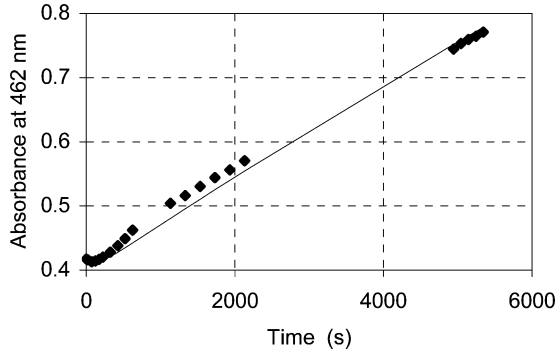

Figure 8. Absorbance at 462 nm vs time for Run C: $[HClO_4]_0 = 0.10$ M, $[I_2]_0 = 0.00056$ M, $[TTA]_0 = 0.020$M, $[IO_3^-]_0 = 0.010$M. Diamonds, experimental; solid line, calculated. Mean standard deviation: 0.012.

OA were present in BZ mixtures or in subsystems and that FA was formed from GOA in BZ mixtures. These same species appear during oxidation of BR products and intermediates by H_2O_2 and Ce^{3+} or Mn^{2+}. Fenton-type reactions proceed through radicals. The iodine-based radicals in the BR system no doubt react differently than bromine-based radicals in the BZ system. In addition, H_2O_2 and O_2 in the BR system can intercept some of the radicals and produce HO• or HOO• and organic peroxy-radicals. It is of course impossible to run oxygen-free BR reactions due to the rapid rate of O_2 evolution.

Conclusions

The main initial product in the BR reaction, IMA, is rather reactive, and undergoes changes during the oscillatory regime. In general, IMA reacts in various ways: with reducing agents to form malonic acid and I^-; and with Hg^{2+} or Ag^+ to form TTA plus an insoluble metal iodide. IMA can also halogenate active unsaturated molecules such as resorcinol. In particular, in an environment similar to that in the BR oscillator (acidic H_2O_2 + Mn(II) or Ce(III) catalyst) the products are OA (most likely through TTA) and I_2. IMA can be iodinated to form I_2MA, which is even more reactive. In that same acidic H_2O_2 + Mn(II) or Ce(III) environment, I_2MA either decarboxylates to I_2AA and CO_2, or is oxidized to OA (most likely through MOA) + I_2 + CO_2. TTA is oxidized by IO_3^- + I_2 to produce MOA. MOA is rapidly oxidized by H_2O_2 + catalyst to produce OA + CO_2. OA is relatively stable under the same conditions, although it is also oxidized to CO_2 on a much longer time scale. Thus, IMA, I_2MA, TTA, and MOA all eventually form OA, which can precipitate $Ce_2(C_2O_4)_3$, decreasing the concentration of the catalyst. GCA and GOA are both oxidized to FA under similar conditions. Because FA is not found in BR mixtures after oscillations, GOA and GCA pathways can be ruled out.

Muntean et al.[17] have shown that IMA is responsible for most of the CO_2 and CO evolution during BR oscillations and that the rate of evolution slows markedly when oscillations cease. We hypothesize that IMA contributes to the oscillation behavior in the BR reaction, partly by providing a source for I^- and I_2, and almost certainly by providing chain carriers for radicals. It is clear that a revised mechanism for the oscillator must include IMA reactions and pathways to CO_2, CO, and oxalic acid.

Acknowledgment. The 300 MHz Bruker Avance NMR spectrometer was purchased using funds from the NSF (DUE 0310554) and Penn State Berks College. We are indebted to an anonymous reviewer for helpful comments and a very careful reading of the manuscript.

References and Notes

(1) Briggs, T. S.; Rauscher, W. C. *J. Chem. Educ.* **1973**, *50*, 496.
(2) Noyes, R.; Furrow, S. D. *J. Am. Chem. Soc.* **1982**, *104*, 45.
(3) De Kepper, P.; Epstein, I. R. *J. Am. Chem. Soc.* **1982**, *104*, 49.
(4) Turányi, T. *React. Kinet. Catal. Lett.* **1991**, *45*, 235.

(5) Vukojevic, V.; Sørensen, P. G.; Hynne, F. J. *J. Phys. Chem.* **1996**, *100*, 17175.
(6) Kim, K. R.; Lee, Dong J.; Shin, K. J. *J. Chem. Phys.* **2002**, *117*, 2710.
(7) Kim, K. R.; Shin, K. J.; Dong, J. *J. Chem. Phys.* **2004**, *121*, 2664.
(8) Furrow, S. D.; Cervellati, R.; Amadori, G. *J. Phys. Chem. A* **2002**, *106*, 5841.
(9) Cervellati, R.; Furrow, S. D. *Inorg. Chim. Acta* **2007**, *360*, 842.
(10) Furrow, S. D.; Höner, K.; Cervellati, R. *Helv. Chim. Acta* **2004**, *87*, 735.
(11) Cervellati, R.; Höner, K.; Furrow, S. D.; Neddens, C.; Costa, S. *Helv. Chim. Acta* **2001**, *84*, 3533.
(12) Lawson, T.; Fülöp, J.; Wittmann, M.; Noszticzius, Z.; Muntean, N.; Szabó, G. *J. Phys. Chem. A* **2009**, *113*, 14095.
(13) Onel, L.; Bourceanu, G.; Wittmann, M.; Noszticzius, Z.; Szabó, G. *J. Phys. Chem A.* **2008**, *1121*, 11649.
(14) Leopold, K. R.; Haim, A. *Int. J. Chem. Kinet.* **1977**, *9*, 83.
(15) Vanag, V. K. *J. Chem. Biochem. Kinet.* **1992**, *2*, 75.
(16) Szabó, G.; Csavdári, A.; Onel, L.; Bourceanu, G.; Noszticzius, Z.; Wittmann, M. *J. Phys. Chem A.* **2007**, *111*, 610.
(17) Muntean, N.; Szabó, G.; Wittmann, M.; Lawson, T.; Fülöp, J.; Noszticzius, Z.; Onel, L. *J. Phys. Chem A.* **2009**, *113*, 9102.
(18) Hansen, E. W.; Gran, H. C.; Ruoff, P. *J. Phys. Chem.* **1984**, *88*, 4908.
(19) Zhabotinsky, A. M. Belousov−Zhabotinsky reaction. *Scholarpedia* **2007**, *2* (9), 1435.
(20) Shaka, A. J.; Keeler, K.; Frenkiel, T.; Freeman, R. *J. Magn. Reson.* **1983**, *52*, 335.
(21) Cobb, R. L. *J. Org. Chem.* **1958**, *23*, 1368.
(22) Kórös, E.; Varga, M. *J. Phys. Chem.* **1982**, *86*, 4839.
(23) Noszticzious, Z.; Ouyang, Q.; McCormick, W. D.; Swinney, H. L. *J. Am. Chem. Soc.* **1992**, *114*, 4290.
(24) Piotto, M.; Saudek, V.; Sklenár, V. *J. Biomol. NMR* **1992**, *2*, 661. Sklenár, V.; Piotto, M.; Leppik, R.; Saudek, V. *J. Magn. Reson Ser. A* **1993**, *102*, 241.
(25) Hansen, E. W.; Ruoff, R. *J. Phys. Chem.* **1988**, *92*, 2641.
(26) Muntean, N.; Szabó, G.; Onel, L.; Lawson, T.; Wittman, M.; Noszticzius, Z.; Furrow, S.; work in progress.
(27) Furrow, S. D. *J. Phys. Chem.* **1995**, *99*, 11131.
(28) Hegedus, L.; Wittmann, M.; Noszticzius, Z.; Yan, S.; Sirimungkala, A.; Försterling, H.-D.; Field, R. J. *Faraday Disc.* **2001**, *120*, 21.
(29) Hoops, S.; Sahle, S.; Gauges, R.; Lee, C'.; Pahle, J.; Simus, N.; Singhal, M.; Xu, L.; Mendes, P.; Kummer, U. COPASI — a COmplex PAthway Simulator. *Bioinformatics* **2006**, *22*, 3067–74.
(30) Schmitz, G. *Int. J. Chem. Kin.* **2004**, (36), 480.
(31) Turner, D. H.; Flynn, G. W.; Sutin, N.; Beitz, J. V. *J. Am. Chem. Soc.* **1972**, *94*, 1554.
(32) Schmitz, G. *Phys. Chem. Chem. Phys.* **2000**, *2*, 4041.
(33) Furrow, S. D. *J. Phys. Chem.* **1987**, *91*, 2129.
(34) Awtrey, A. D.; Connick, R. E. *J. Am. Chem. Soc.* **1951**, *73*, 1842.
(35) Allen, T. L.; Keefer, R. M. *J. Am. Chem. Soc.* **1955**, *77*, 2957.
(36) Dushman, S. *J. Phys. Chem.* **1904**, *8*, 453.
(37) Ruoff, P.; Hansen, E. W.; Noyes, R. M. *J. Phys. Chem.* **1987**, *91*, 3393.
(38) Györgyi, L.; Turányi, T.; Field, R. J. *J. Phys. Chem.* **1990**, *94*, 7162.
(39) Hegedüs, L.; Försterling, H. D.; Wittmann, M.; Nosztizcius, Z. *J. Phys. Chem. A.* **2000**, *104*, 9914.
(40) Onel, L.; Bourceanu, G.; Bitter, I.; Wittmann, M.; Nosztizcius, Z. *J. Phys. Chem. A.* **2006**, *110*, 990.
(41) Onel, L.; Wittmann, M.; Pelle, K.; Nosztizcius, Z.; Sciascia, L. *J. Phys. Chem. A.* **2007**, *111*, 7805.

JP911492F